Molecular Crystals and Liquid Crystals

Publication details, including instructions for authors and subscription information:
http://www.tandfonline.com/loi/gmcl20

The LCPDI: A Compact and Robust Phase-Shifting Point-Diffraction Interferometer Based on Dye-Doped LC Technology

Kenneth L. Marshall [a], Kathleen Adelsberger [a], Graham Myhre [a] & DeVon W. Griffin [b]

[a] Laboratory for Laser Energetics, University of Rochester, Rochester, New York, USA

[b] NASA Glenn Research Center, Microgravity Fluid Physics Branch, Brookpark, Ohio, USA

Version of record first published: 22 Sep 2006

To cite this article: Kenneth L. Marshall, Kathleen Adelsberger, Graham Myhre & DeVon W. Griffin (2006): The LCPDI: A Compact and Robust Phase-Shifting Point-Diffraction Interferometer Based on Dye-Doped LC Technology, Molecular Crystals and Liquid Crystals, 454:1, 23/[425]-45/[447]

To link to this article: http://dx.doi.org/10.1080/15421400600654116

Mol. Cryst. Liq. Cryst., Vol. 454, pp. 23/[425]–45/[447], 2006

ISSN: 1542-1406 print/1563-5287 online
DOI: 10.1080/15421400600654116

Taylor & Francis
Taylor & Francis Group

The LCPDI: A Compact and Robust Phase-Shifting Point-Diffraction Interferometer Based on Dye-Doped LC Technology

Kenneth L. Marshall
Kathleen Adelsberger
Graham Myhre
Laboratory for Laser Energetics, University of Rochester, Rochester, New York, USA

DeVon W. Griffin
NASA Glenn Research Center, Microgravity Fluid Physics Branch, Brookpark, Ohio, USA

Point-diffraction interferometers, by design, are much less sensitive to environmental disturbances than dual-path interferometers, but, until very recently, have not been capable of phase shifting. The liquid crystal point diffraction interferometer (LCPDI) utilizes a dye-doped, liquid crystal (LC), electro-optical device that functions as both the point-diffraction source and the phase-shifting element, yielding a phase-shifting diagnostic device that is significantly more compact and robust while also using fewer optical elements than conventional dual-path interferometers. These attributes make the LCPDI of special interest for diagnostic applications in the scientific, commercial, military, and industrial sectors, where vibration insensitivity, power requirements, size, weight, and cost are critical issues.

Until very recently, LCPDI devices have used a plastic microsphere embedded in the LC fluid layer as the point-diffraction source. The process for fabricating microsphere-based LCPDI devices is low-yield, labor-intensive, very "hands-on," and great care and skill are required to produce devices with adequate interference fringe contrast for diagnostic measurements. With the goal in mind of evolving the LCPDI beyond the level of a laboratory prototype, we have developed "second-generation" LCPDI devices in which the reference diffracting elements are an

This work is supported by the U.S. Department of Energy Office of Inertial Confinement Fusion under Cooperative Agreement No. DE-FC52-92SF19460 and the University of Rochester. The support of DOE does not constitute an endorsement by DOE of the views expressed in this article. This work was also supported by the NASA Glenn Research Center Microgravity Fluid Physics Division under Grant # NAG3-2348.

Address correspondence to Kenneth L. Marshall, Laboratory for Laser Energetics, University of Rochester, 250 East River Road, Rochester, NY 14623, USA. E-mail: kmar@lle.rochester.edu

integral part of the substrates by depositing a suitable optical material (vapor-deposited thin films or photoresist) directly on the substrate surface. These "structured" substrates eliminate many of the assembly difficulties and performance limitations of previous LCPDI devices as well as open the possibility of mass-producing LCPDI devices at low cost by the same processes used to manufacture commercial LC displays.

Keywords: interferometry; liquid crystal; phase-shifting; photoresist; point diffraction

I. INTRODUCTION

Phase-shifting interferometers, which generally utilize separate test and reference beams, represent the most accurate and effective way to measure changes in optical path length. One disadvantage is that their large size and extreme sensitivity to mechanical shock, vibration, temperature fluctuations, and air turbulence greatly limit their application in many sensing and monitoring applications. Phase-shifting interfereometers function by changing the optical path difference (OPD) between the sample and reference paths of the interferometer in discrete steps that are equal fractions of a wavelength. When the unchanged wavefront from the reference path is combined with the wavefront that has passed through the test section, the differences in the optical path produce interference fringes. In Mach–Zehnder and Twyman–Green interferometers, the OPD is changed using a piezoelectric actuator to physically move the mirror from a central position in a sinusoidal fashion. This motion changes the OPD and thus the appearance of the resulting interference fringes. The changes in the position of the fringes are imaged on a detector (e.g., a CCD camera) and stored in either computer memory or on a hard storage medium such as a disk or videotape. The optical path is determined using the intensity at each pixel as a function of phase step. To obtain stable fringes, the alignment of both the test and reference paths must be maintained to within a fraction of the wavelength of the light being used for the measurement. Otherwise, the fringes will shift and may disappear. The extreme sensitivity of these interferometers to bumping, jarring, and transmitted vibration means that they must be operated on optical isolation tables in a relatively stable environment to ensure that accurate and reliable interferometric data are obtained.

Point-diffraction interferometers (PDI), where the test and reference beams traverse a common path, are much less vibration-sensitive than the traditional interferometers described above. In the PDI, light passing through the test section is focused onto a small diffracting

object that is typically either a circle of material on a high-quality, semitransparent glass plate or a small sphere in a glass cell. The PDI has the advantage of being substantially more compact and mechanically robust than conventional phase-shifting interferometers, but, until very recently, it was incapable of phase-shifting measurements because it was composed primarily of *passive* optical materials (e.g., glass). Mercer and Creath added phase-shifting capability to the PDI by replacing the point-diffraction source and the passive, semitransparent filter of the conventional PDI with a liquid crystal (LC) electro-optical device containing microspheres embedded in the nematic liquid crystal fluid layer [1,2] (Fig. 1). An incident beam focused on the area of the LC cell that contains an isolated microsphere undergoes optical interference, which occurs as different portions of the beam pass through the microsphere (the reference beam) and the liquid crystal fluid. Because the area of the beam that passes through the LC fluid (the test beam) is substantially larger than the microsphere, the portion of the beam that passes through the LC fluid "host" is attenuated by incorporating an optically absorbing "guest" dye in the LC "host" to obtain high-contrast interferograms. For a 22-μm-thick LCPDI device with a central element that is approximately 1.5 to 2 times the cell thickness, an OD of around 2 is required. Application of an ac drive voltage to the LC device changes its birefringence, which induces phase shifting.

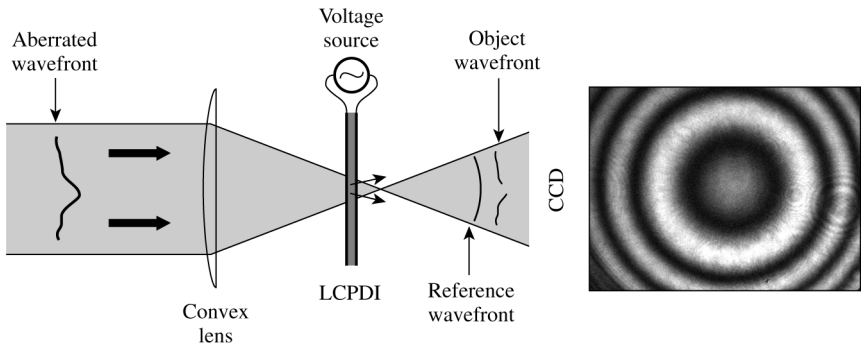

FIGURE 1 Schematic diagram of the LCPDI. The laser beam is focused onto an area of the liquid crystal electro-optic device containing a glass or plastic sphere in the LC fluid gap. The portion of the beam passing through the microsphere functions as the reference arm of the interferometer. Application of an electric field to the birefringent LC material produces controlled molecular reorientation with subsequent generation of interference fringes. Also shown are interference fringes obtained from a typical LCPDI device.

Because both the object and reference beams follow the same path, the LCPDI is relatively insensitive to the mechanical vibrations, temperature fluctuations, and air turbulence that plague conventional phase-shifting interfereometers. Mercer, Creath [3], and Rashidnia [4] first demonstrated the superior stability and robustness of the LCPDI in comparing its performance to that of a phase-shifting Mach–Zehnder interferometer. In later work, Guardalben *et al*. [5] compared the performance of an LCPDI to that of a Zygo Mark IVxp Fizeau phase-shifting interferometer and found that the two techniques yielded measurements on the same witness sample that were in remarkably close agreement.

The compact size, near-solid-state robustness, low voltage/power requirements ($1.5\,V_{rms}$ and nanoamps, respectively), and near-video frame-rate data acquisition potential of the LCPDI concept – *all at a fraction of the cost and size of conventional phase-shifting interferometers* – makes it an extremely attractive diagnostic for challenging applications in the military, commerce, physical sciences, and aerospace environments where physical size, robustness, vibration insensitivity, rapid data collection capability, low power consumption, and low cost are all of critical importance. Unfortunately, the devices described in previous efforts were found wanting in several key performance areas. The low purity of commercial dye dopants produced speckle and fringe instability, time-dependent hysteresis in the electro-optical response, and anomalous and irreversible changes in LC molecular alignment. The high absorbance dichroism of the dye dopants caused the interference fringe contrast to be highly dependent on the applied voltage. Spatial noise generated by defects in conductive coatings, LC polymer alignment coatings, microsphere defects, and extrinsic particulate contamination was also a significant issue. Device-to-device performance was highly inconsistent because the LCPDI phase-shifter fabrication methodology required substantial manual dexterity and skill, was difficult to control, and device yields were poor. As a direct result of an extended research effort at the University of Rochester [6,7], funded by both the U.S. Department of Energy and NASA's Microgravity Fluid Physics Division, nearly all of these materials and manufacturing issues for LCPDI modulators employing microspheres as the diffractive reference element were addressed successfully and it became possible to fabricate these "first-generation" LCPDI devices in sufficient quality and quantity to begin seriously evaluating their potential as a useful diagnostic instrument.

In pursuing this development effort, it became quite clear to us that no matter how well the fabrication process for first-generation,

microsphere-based LCPDI's was optimized, there would always be reproducibility and yield limitations. The main reason for these limitations is that each device must be "hand-built," and, as such, the device quality inherently depends on the skill, concentration, and patience of the individual assembler. For the LCPDI to achieve the robustness, uniformity, and device-to-device performance consistency required for them to be widely accepted as a useful diagnostic tool, *they must be able to be manufactured reproducibly and cost-effectively in large quantities*. With this goal in mind, we have developed a "second-generation" LCPDI device in which *the reference diffracting elements and spacers are an integral part of the substrates* through the deposition of a suitable optical material directly on the substrate surface. These "structured" substrates eliminate many of the assembly difficulties and performance limitations of first-generation LCPDI devices and open the possibility *of mass-producing LCPDI devices at low cost by the same processes used to manufacture commercial LC displays*.

In this paper, we will overview the materials-related challenges that were met and overcome on the road to fabrication of the first-generation LCPDI devices, review the current state of the art of these microsphere-based, first-generation LCPDI devices, and describe the first successful prototype devices based on structured substrates that both demonstrate the feasibility of the approach and represent a major step forward toward the goal of producing high-quality, second-generation LCPDI devices for practical applications.

II. LCPDI APPLICATION AREAS

In early 2000, a collaborative research effort was initiated between the University of Rochester's Laboratory for Laser Energetics (LLE) and the NASA Glenn Research Center to study the key materials and device issues for developing the LCPDI device into a reliable and useful tool both for use in microgravity fluid physics research at NASA and as a beamline diagnostic for the 60-beam, 40-terawatt, 1054-nm OMEGA Laser System used in the Department of Energy's inertial confinement fusion research at LLE. The goal of the research was to develop materials systems and fabrication methods that would lead to highly precise LCPDI devices of consistent quality for both DOE and NASA research efforts, with the long-term goal leading to devices that could be manufactured in a cost-effective manner for other applications in the scientific, commercial, military, and industrial sectors. In this section we briefly describe these applications and their requirements.

Difficulties in manufacturing the large-aperture optical elements used in the OMEGA system add aberrations to each laser beam that

can result in wavefront errors in the incident beams. Such wavefront errors can manifest themselves in unequal illumination of the target, which, in turn, reduces the uniformity of the energy being delivered by the laser. Although numerous diagnostic instruments are used on OMEGA to analyze problems with beam uniformity, a more effective method of measuring wavefront aberrations at 1054 nm than what is currently available is required. Shearing interferometery is currently used to analyze OMEGA beamlines, but the method suffers from (1) an inability to perform gradient measurements in more than two directions, (2) a low sensitivity to high-order phase errors, and (3) low spatial resolution. The large physical size and the need for vibration isolation makes conventional near-IR phase-shifting interferometers impractical for these characterization activities, as each of the 60 beams would have to be propagated a long distance across free space to reach the interferometer table. The LCPDI would solve the problem as its small size, light weight, and vibration insensitivity would allow it to be moved from beamline to beamline as needed.

Fluid management and fundamental science in microgravity remains an active area of research for NASA's mission of space exploration. Research topics include such diverse areas as thermocapillary flow [8,9], nucleate boiling [10], and diffusion of miscible fluids [11]. In all of these research areas, there is a need to visualize or measure the mixing or temperature response of transparent liquids. Visible-region interferometry at 543 nm is the technique of choice for many such measurements. In terrestrial-based experiments where size, weight, and power are not critical issues, the use of conventional phase-shifting interferometers mounted on large vibration isolation tables is not a barrier. But for extraterrestrial experiments, severe volume, power, and mass constraints along with the lack of vibration isolation suggest phase-shifting, common-path interferometry using the LCPDI as an extremely attractive and viable solution. In thermocapillary flow studies in enclosed chambers, the LCPDI's potential to capture interferometric data at video frame rates along with its small size would make tomographic measurements on turbulent phenomena possible – an experiment that, to date, has only been accomplished by using the lower resolution Hartmann–Shack wavefront sensors [12].

III. LCPDI DEVELOPMENT CHALLENGES

Early LCPDI devices suffered from a number of performance limitations, including excessive fringe noise, a substantial reduction in contrast with applied voltage, speckle produced by electrohydrodynamic effects in the dye-doped liquid crystal material, and device-to-device

performance inconsistencies due to fabrication methodology, coating defects, extrinsic particle contamination either on the microspheres or in the LC material, and entrained air bubbles in the device – all resulting in spatial noise in the fringe data. For these microsphere-based devices, the fabrication technique required the microspheres to be placed on the substrates *by hand* using a high-power microscope. Because the microspheres are held in place only by surface static charges, they are easily dislocated and will scratch the LC alignment layer when the second substrate is placed unless exceptional care is taken during cell assembly.

As a result of our extensive LCPDI development investigations, we determined that the two areas in which improvements would most greatly impact LCPDI performance were in (1) the liquid crystal guest–host dye formulations and (2) device fabrication methodology. The following sections outline the most recent progress made in these two areas.

IV. LIQUID CRYSTAL MATERIALS AND DYES

The LC "host" material used in LCPDI devices is Merck E7, a well-known and mature commercial room-temperature nematic LC mixture of cyanobiphenyl and cyanoterphenyl compounds with relatively high birefringence (Δn), large positive dielectric anisotropy ($\Delta\varepsilon$), and a broad nematic phase range. This material has a long history of use as a host for dichroic dyes of widely varying structures, making it the most practical candidate for the LCPDI.

Dyes that are suitable for use in an LCPDI device must meet stringent requirements. They must have both large absorbance oscillator strength at or near the desired operating wavelength and good LC host solubility. Their impact on the LC host mixture order parameter must be minimal to achieve sharp, high-contrast interference fringes. Low electrical conductivity is required to avoid unwanted electrohydrodynamic effects (e.g., speckle and scattering). Little or no electric field-induced absorbance dichroism in the guest–host mixture is also extremely important to achieve fringes with constant contrast. *No single commercial dye or group of dyes was found to be able to meet all of these requirements*. Commercially available visible-region dyes suitable for direct use in LC hosts are highly dichroic because the largest single market for LC guest–host dyes is in the information display industry, which requires dyes with a large (positive or negative) dichroic ratio. Other commercial visible-region dyes (e.g., textile dyes or oil-soluble dyes) were found to be so impure as to be nearly useless in LC materials without first undergoing extensive purification.

Design and synthesis of a totally new dye with an extremely small or nonexistent dichroism, although of great interest from the chemical synthesis point of view, was simply not practical because of limitations in time and resources. Alternatively, we took a more practical, cost-effective, and somewhat novel approach to the dichroism issue by combining dyes with a positive or negative dichroism in appropriate ratios into the LC host to compensate for changes in absorption with applied electric field. These "*contrast-compensated*" guest–host mixtures effectively solved the voltage-dependent contrast problem.

From the large number of commercially available visible-region positive dichroic dyes we chose Oil Red O [Fig. 2(a)] as the positive dichroic component. Because all of the few available negative dichroic dyes tested drastically increased the LC guest–host mixture conductivity and induced homeotropic LC alignment with time or elevated temperature, we synthesized a series of alkyl substituted ester/amide dyes based on diamino dihydroxyanthraquinone compounds that had been identified in the literature [13–15] as excellent negative dichroic dye candidates for LC hosts. The generic chemical structure of this dye series is shown in Figure 2(b). Although compounds with terminal alkyl chains ranging from C_5 to C_9 were synthesized, the C_9 derivatives were not used for mixture formulation because of the low yield and great difficulty in purification of this material.

Of fifteen dye mixtures originally formulated, only three formulations were found to have sufficient compositional stability (resistance to crystallization), low electrical conductivity, and sufficient OD to be useful for LCPDI devices. These mixtures and their properties are listed in Table 1. Generally, a total dichroic dye concentration (including both positive and negative dyes) of between 3 and 5 wt% is needed

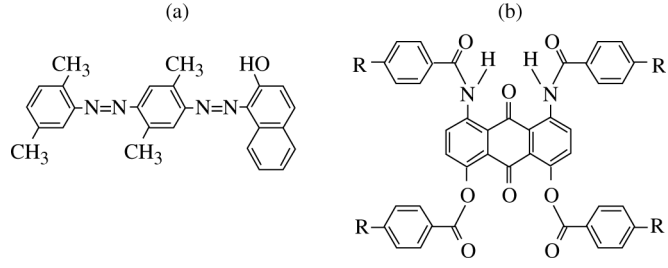

FIGURE 2 The molecular structures of dichroic dyes used in the "Contrast-compensated" dye-doped mixture for the LCPDI (a) Oil Red O, a positive dichroic dye; (b) the generic structure for the anthraquinone dyes with negative dichroism. The "R" groups range from C_5 to C_9.

TABLE 1 Contrast-Compensated Dichroic Dye Mixtures Developed for the LCPDI Device

Mixture composition (in 1 g of E7)				Electrical properties*				
Total dyes (wt%)	Negative dichroic dyes	Positive dichroic dyes	Dichroic ratio (+:−)	Capacitance (nF)	Resistance (kΩ)	OD* (0 V)	OD* (10 V)	OD ratio
3.5	C5 (7 mg) C6 (7 mg) C7 (7 mg) C8 (7 mg)	Oil Red O (7 mg)	80:20	1.2	73.3	2.13	1.42	0.71
5.1	C5 (8 mg) C6 (8 mg) C7 (8 mg) C8 (20 mg)	Oil Red O (7 mg)	86.3:13.7	1.2	72.7	2.05	1.72	0.33
5.35	C5 (7.5 mg) C6 (7.5 mg) C7 (7.5 mg) C8 (20 mg) Orasol Red (2 mg)	Oil Red O (9 mg)	83.2:16.8	10.9	5.7	3.00	2.39	0.61

*Measured in a 22-μm path cell, 543-nm, 1-khz applied field.

to achieve the OD of ≥ 2 required for sharp, high-contrast interference fringes in a 22-μm path LCPDI cell. This critical path length value is the largest that can be used without substantially increasing the LCPDI device response time.

For the near-IR region of the spectrum, the selection of potential dye candidates for an LCPDI intended to operate near 1054 nm is severely limited to ~10 to 20 materials. Most of these dyes are designed for laser applications (e.g., *Q*-switching) and are ionic or highly polar. As a result, they show very poor solubility in liquid crystal hosts (0.01 to 0.05 wt%). The low solubility of these dyes in LC hosts limits their maximum blocking efficiency to an OD of < 0.1 at a path length of 25 μm – *two decades less than is required for producing acceptable fringe contrast for diagnostic purposes*.

We addressed this issue by synthesizing a series of zerovalent transition metal dithiolene complexes which from our previous work [16,17] and the work of others [18,19] were known to (1) have strong absorption bands in the 600 to 1500 nm region, (2) be highly soluble in liquid crystal hosts, and (3) could be designed to possess liquid

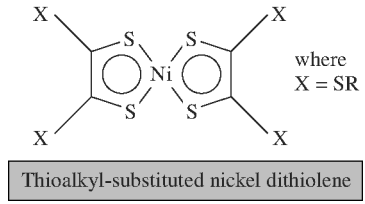

FIGURE 3 The molecular structure of highly soluble zerovalent nickel dithiolene dyes for near-IR LCPDI devices. The "X" groups are thioalkyl substituents with varying chain lengths and substituent positions.

crystalline properties if appropriate terminal functional groups are selected. The latter is a distinct advantage in that it would allow higher concentrations of the dye to be added to the liquid crystalline host without substantially reducing its order parameter. Our investigations focused on compounds using nickel as the central transition element with thioalkyl terminal substituents (Fig. 3). Figure 4 shows the electro-optic behavior of a mixture of nine of these dyes in Merck E7. This new series of dyes shows a small degree of *negative* dichroism whereas the materials synthesized previously showed only *positive* dichroism. The mixture easily exceeds the required OD of 2 at 1054 nm in the off-state at a 10-μm path length. Further compensation of the dichoism is possible with the addition of existing positive dichroic nickel dithiolenes.

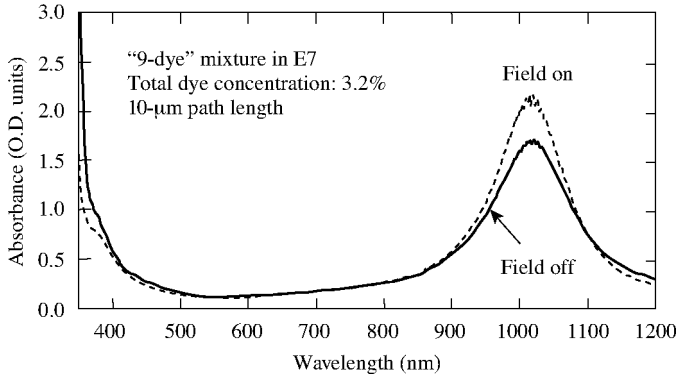

FIGURE 4 The electro-optical performance of a mixture of nickel dithiolene dyes in Merck E7 liquid crystal. The required OD of 2 at 1054 nm is easily achieved at a 10-μm path length. The dye-doped mixture displays a small amount of negative dichroism (the absorbance increases when the electric field is applied).

V. "FIRST-GENERATION" LCPDI USING MICROSPHERES AS DIFFRACTIVE ELEMENTS

Figure 5 shows a diagram of the first-generation LCPDI modulation element employing microspheres as both the diffractive reference element and the spacers for controlling the LC fluid gap thickness based on the original device concept proposed by Mercer and Creath. This "first-generation" device contains a deformable plastic microsphere as the reference beam diffraction element held in compression between two transparent $25\,\text{mm} \times 25\,\text{mm} \times 3\,\text{mm}$ glass substrates. The inner substrate surfaces are coated with a 500-Å layer of indium–tin oxide (ITO) as a conductive coating. This ITO layer is overcoated with a 250-Å layer of a spin-deposited polymer coating that has been mechanically treated to produce a preferred orientation direction for the LC molecules when the cell is filled. A UV-curing epoxy containing plastic microspheres whose diameter is slightly less than that of the reference microspheres is used to bond the substrates together near the corners and maintain compression on the reference microsphere element. Experimental evidence has shown that that the best results are obtained when the diameter of the polymer reference

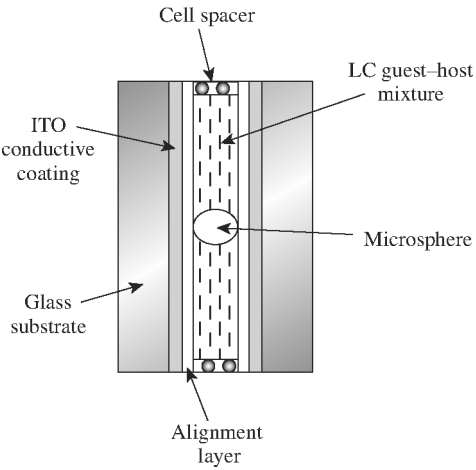

FIGURE 5 Diagram of a "first-generation" LCPDI modulator device that employs microspheres for both the reference diffractive element and as cell spacers. In the latter case, the microspheres are dispersed in a UV-curing epoxy formulated and applied as spacer "pads" near the edges of the substrates before assembly.

microspheres *before compression* is 1.5 to 2× larger than the intended cell gap.

V.A. Alignment Coatings

Uniform LC molecular alignment in first-generation LCPDI devices was generated by the industry-standard process of mechanically buffing a spin-deposited polymer coating (either Nylon 6/6 or polyimide) with a velvet roller. Polyimide was ultimately selected as the material of choice for buffed alignment coatings because of its superior adhesion to the ITO-coated substrates, which minimized alignment coating damage in the event that the microspheres were displaced slightly during device assembly.

V.B. Device Assembly Procedures

Alignment coating defects, extrinsic particle contamination, and air bubbles in the vicinity of the reference elements will all produce spatial noise in the interference fringe data. High-quality, defect-free devices, were obtained by conducting all device fabrication processes in a Class 100 clean room environment, with final assembly done in a Class 10 vertical laminar-flow clean hood contained within the Class 100 clean area. All LC materials and coating solutions were microfiltered to 0.2 μm. Both the substrates and microspheres were rigorously cleaned to eliminate foreign contaminants. The microspheres used as reference diffraction elements (1.5 to 2× larger than the intended cell path length) were placed by hand in a widely separated, diamond-shaped pattern near the center of the clear aperture of the cell with the aid of a high-power optical microscope housed within the Class 10 hood. Microspheres with diameters equal to the desired cell gap spacing were dispersed into a UV-curing adhesive and applied to the inner coated surfaces of the substrates near each of the four corners. The substrates were carefully joined together without dislocating the microspheres using a specially designed fixture. Sufficient pressure was applied to compress the reference microspheres, and the UV-curable adhesive was irradiated to bond the substrates. Upon successful completion of the bonding process, the cell was filled by capillary action with the dye-doped LC mixture and edge-sealed with the same UV-curing adhesive. The bonding of wire leads to the LCPDI device using a conductive epoxy formulation completed the assembly process. A completed LCPDI device is shown in Figure 6 with a representative fringe pattern from one of the first devices fabricated successfully using the optimized process.

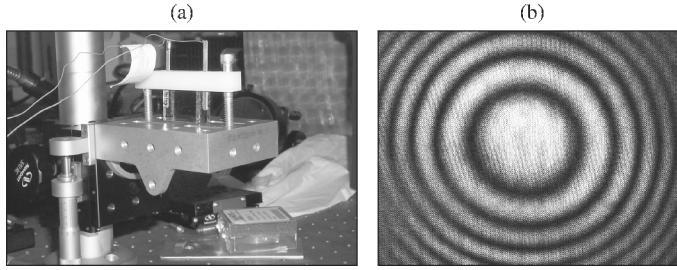

FIGURE 6 (a) A completed 22-μm-thick LCPDI device, mounted in a positioning stage and ready for evaluation; (b) fringe pattern from one of the first LCPDI devices fabricated successfully using the optimized assembly process.

V.C. Relationship of Applied Voltage to Phase Shift

The dependence of phase shift on applied voltage was determined using a Soleil compensator setup. A polarized HeNe laser and a PIN photodiode with a rotatable analyzer were used as the light source and detector, respectively. The LCPDI device was placed between the Soliel compensator and the analyzer, the retardance of the Soleil compensator was set at 0, and the analyzer polarization was set parallel to the laser polarization. A series of fixed ac voltage levels were generated by a Stanford Research Systems DS345 30-MHz synthesized function generator and applied to the LCPDI device and the amount of the electrically-induced phase shift was determined by adjusting the Soleil compensator to achieve an optical minimum on the detector. Figure 7 shows curves for calculated and normalized phase-shift data plotted on a common axis as a function of voltage for a 22-μm-thick, first-generation LCPDI device. The response curve over the full voltage range is highly nonlinear, as is expected because of the quadratic nature of the response of the LC material to the ac field; however, because small increments of applied voltage produce substantial phase shifts, it is easily possible to find sections of the response curve to operate the LCPDI device where the phase shift with applied voltage is linear and predictable.

This voltage versus phase-shift data can be used as a calibration curve for the LCPDI modulator by entering it into a look-up table in the software portion of a suitable LCPDI electronics driver package (currently under development), allowing direct selection of the desired phase-shift interval from a computer-based graphical user interface.

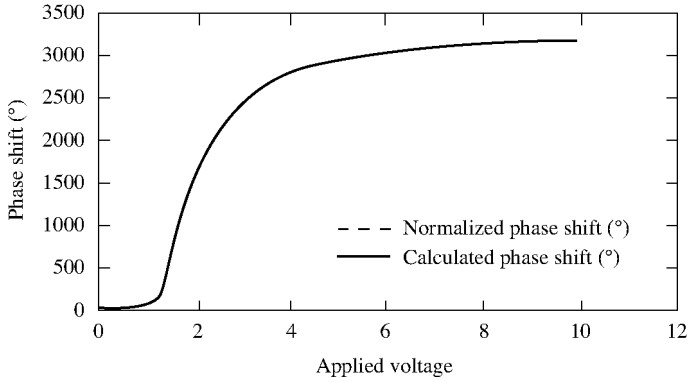

FIGURE 7 Normalized and calculated phase-shift data as a function of voltage for a 22-μm-thick LCPDI device. Although the magnitude of the electrically induced phase shift is highly nonlinear over the entire voltage range, its efficiency per unit voltage is so large that only small sections of the total curve need to be used in order to achieve linear and predictable phase shifting.

V.D. Phase Shifting in ''First-Generation'' LDPDI Devices

Fabricated first-generation LCPDI devices were characterized for their fringe quality and phase-shifting capability using an interferometer setup based on that shown in Figure 8. The interferometer setup is a straight-line design employing 1-in. optics, with the entire length of the setup utilizing the full length of a 3-m optical table. The LCPDI device is mounted with its molecular alignment axis parallel to the laser polarization in a custom-made rotating holder

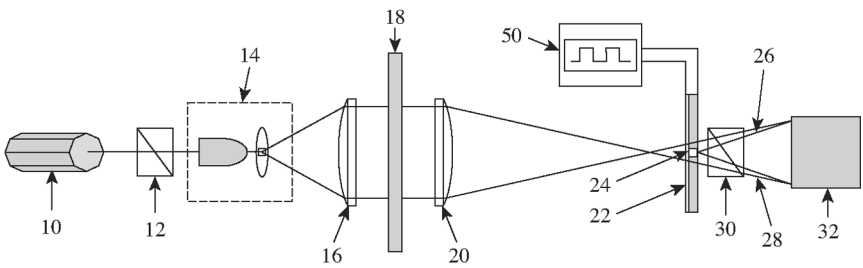

FIGURE 8 A schematic representation of the LCPDI interferometer test setup: Green He Ne laser (10), polarizer (12), spatial filter (14), collimating lens (16), sample under test (18), focusing lens (20), LCPDI device (22), microsphere reference element (24), optional analyzer (30), sample wavefront (28), reference wavefront (26), Micropix IEE 488 Firewire CCD camera (32), SRS synthesized function generator, and HP digital oscilloscope (50).

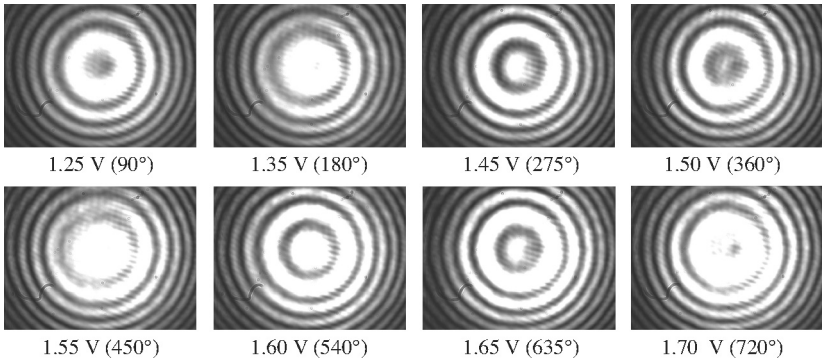

FIGURE 9 Phase-shifting interferograms taken from Device KA-26 (5.1% total dye concentration, LPP "photobuffed" alignment coating, 22-μm cell path length). A manually ramped 5-KHz sine wave was used as the driving waveform. This set of interferograms shows two complete 360° phase shifts.

that, in turn, is mounted on a precision three-axis stage. The stage is adjusted until the interference fringes from the reference diffractive element are properly imaged at the focal plane of the Micropix IEEE 1394 Firewire CCD camera. The supplied camera software allows either single frame images (Micropix) or image streams (Stream-Pix) to be captured directly to disk at frame rates as high as 30 frames/sec. sec. Data was acquired by either applying a static ac voltage and capturing individual frames or applying a voltage ramp or spike and acquiring a free-running image stream at a selected acquisition rate. Figure 9 shows phase-shifting interferograms obtained using a first-generation LCPDI containing a contrast-compensated dye mixture at 5.1% dye concentration. The LCPDI modulator was driven with a 1 to 5 kHz sine waveform with voltage levels manually ramped from the front panel of the SRS function generator. This set of interferograms shows two complete 360° phase shifts.

VI. "SECOND-GENERATION" LCPDI DEVICES USING "STRUCTURED" SUBSTRATES

The formation of structured substrates by deposition of a suitable optical material directly on the substrate surfaces makes the reference-diffracting elements and spacers an integral part of the substrates and eliminates many of the assembly difficulties and performance limitations of first-generation LCPDI devices [20]. Potential mass production of LCPDI devices at low cost now becomes a viable

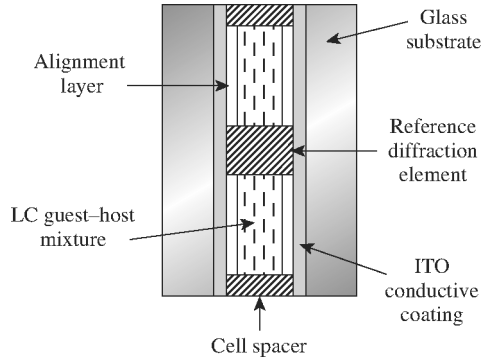

FIGURE 10 Second-generation LCPDI device using one "structured" substrate and one plain (unstructured) substrate.

option because the envisioned process utilizes many of the same steps used in the manufacture of commercial LC displays. Figure 10 shows a cross sectional view of a device composed of one "structured" substrate and one plain (unstructured) substrate sandwiched together to make an LCPDI device. Because the diffractive elements and spacers are integral to the substrate, assembly of the device is greatly facilitated. For this device form, the cell thickness is limited to the height of the structural feature(s) that can be applied to a single substrate. A perspective view of the two substrates is shown in Figure 11. Although, in principle, a pair of identically structured substrates could be used to assemble LCPDI devices with larger LC path lengths, this approach

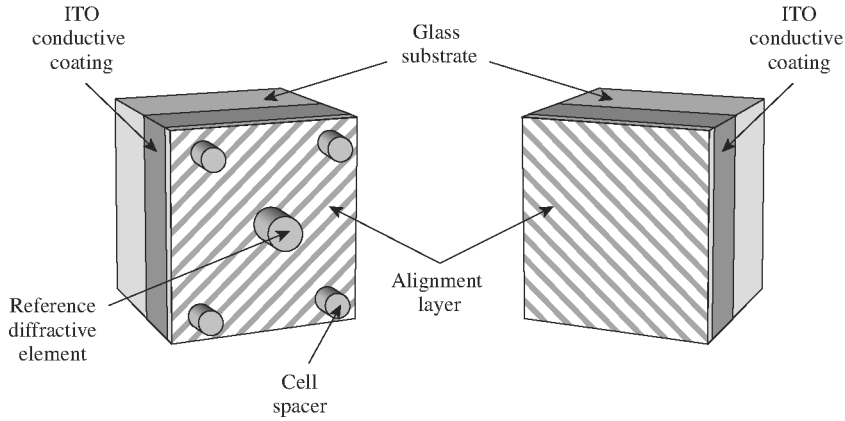

FIGURE 11 Perspective view of the substrates used in the second-generation LDPDI device shown in Figure 10.

introduces considerable complexity in the assembly process, as the structural features on the two substrates will need to be carefully aligned (registered).

We investigated two deposition approaches for fabrication of structured substrates: (1) vapor-deposited inorganic thin films and (2) photolithographic patterning of a spin-deposited photoresist layer.

VI.A. Vapor Deposition of Inorganic Thin-Film Structures

Tantalum pentoxide (Ta_2O_5) diffractive-reference elements and LC fluid gap spacers were vapor-deposited onto ITO-coated glass substrates (1-in.$\times$1-in.) in the LLE Optical Manufacturing Group's thin-film coating facility. The diffractive elements and cell spacers were evaporated through a machined aluminum fixture with four 4-mm apertures that define the spacers and one 9.5-mm aperture that defined the reference diffractive element. The 9.5-mm aperture holds an aluminum foil mask containing a precision-drilled hole approximating the diameter of the reference diffractive element to be evaporated (45 to 100 μm). The ITO-coated substrate was mounted in the fixture, and the assembly was placed in a 28-in. electron-beam evaporation system with an 8-cm ion source at 2×10^{-6} Torr. After precleaning the ITO surface for 5 min with an argon ion beam, Ta_2O_5 was deposited at 200°C at a deposition rate of ~ 4 Å/s, monitored by a single-wavelength optical monitor (650 nm) operating in transmission mode. The deposition of Ta_2O_5 was continued until a sufficient number of quarter-wave optical thicknesses had been deposited (22 quarter-wave thicknesses = 5 μm).

Figure 12 shows a New View optical profilometer scan of a 100-μm-diam vapor-deposited Ta_2O_5 central diffractive element vapor-deposited onto an ITO-coated substrate at a 14-μm step height. At the large step heights required to achieve good fringe contrast, both the cross sectional profile and its height accuracy of the Ta_2O_5 structural element is severely compromised. The ragged cross sectional profile of the diffractive element deposited at a 14-μm thickness, and its substantially reduced height (9 μm) after completion of the evaporation and removal of the substrate from the fixture is due to damage caused by adhesion of a portion of the evaporated element to the mask. This problem occurred regularly in test runs for step heights exceeding 10 to 12 μm.

VI.B. Photoresist Patterning Structures

Photoresist patterning was accomplished at the Rochester Institute of Technology's Semiconductor & Microsystems Fabrication Laboratory

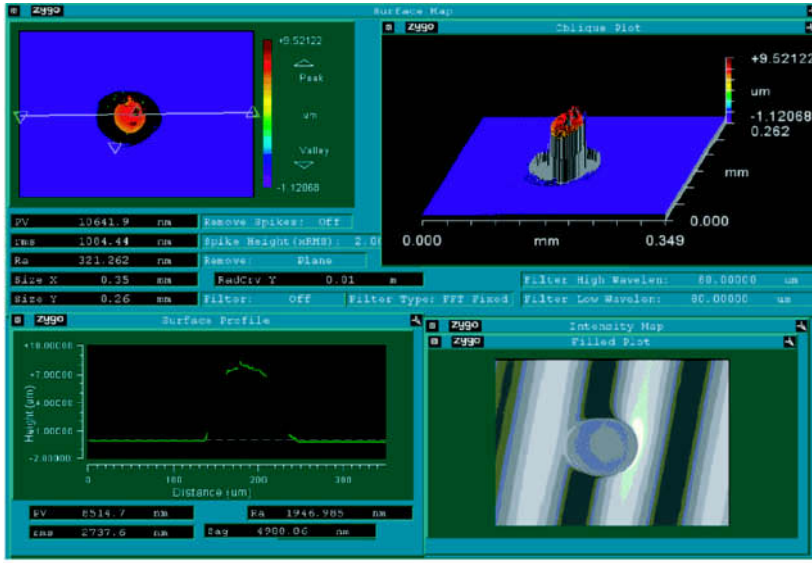

FIGURE 12 New View optical profilometer scans of 100-μm-diam vapor-deposited Ta_2O_5 central diffractive elements on ITO-coated substrates deposited at a 14-μm step height.

(SMFL) using laser-drilled precision pinholes mounted in a special fixture on a Karl Suss precision contact mask aligner. MicroChem Corp. SU8-2010, a negative photoresist formulation that is both optically transparent at 543 nm and chemically compatible with both the LC material and the alignment coating materials, was spin-deposited onto the LCPDI substrates prior to patterning. The diameter of the pinhole controlled the diameter of the diffraction element patterned in the photoresist (a 50-μm pinhole produces an element with a 60-μm diameter), while the spin deposition parameters along with the content of the photoresist solution controlled the element height. Diffraction element heights of between 17 and 22 μm were reproducibly achieved. Figure 13 shows a New View optical profilometer scan of a single diffractive element patterned in SU8-2010 photoresist on an ITO coated substrate. A 17-μm step height is easily achieved with an excellent cross sectional profile and overall uniformity.

VI.C. Alignment Layer Deposition on Structured Substrates

The application and processing of LC alignment layers onto structured substrates presented a significant challenge. Conventional mechanical

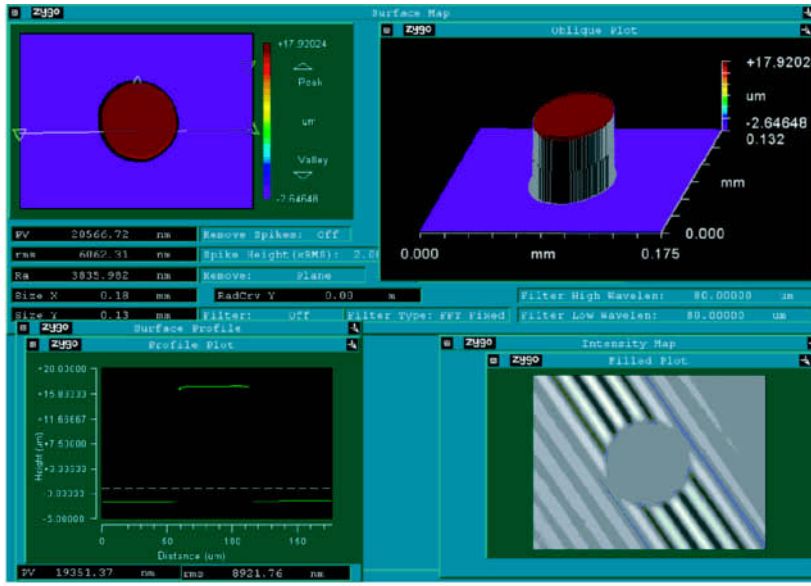

FIGURE 13 New View optical profilometer scan of a diffractive element patterned in SU8-2010 photoresist on an ITO-coated substrate.

buffing techniques for generating LC alignment cannot be used in this case because of the potential for damaging or completely removing the micron-sized structural features by the inherent shear forces. We overcame this problem by employing LC alignment technology based on *linear photopolymerizable polymers* (LPP), in which the preferred LC alignment direction is generated *photochemically* using polarized UV light. Although these materials have been under development for many years, it has only been very recently that they have become commercially available. This "photobuffing" process has a number of significant advantages for LCPDI-structured substrate devices: (1) the alignment mechanism is *noncontacting* (no damage to micron-sized structural features), (2) the process is inherently clean – neither extraneous particles are generated nor is there any electrostatic charging that can attract particulates, and (3) the equipment and process are compatible with the Class 10 clean room conditions required for LCPDI device final fabrication.

The LPP material ROP-203/2CP was supplied by Rolic (Switzerland) as a predissolved solution in cyclopentanone. Spin deposition and irradiation parameters for generating high-quality alignment were first developed on standard ITO-coated substrates and

then later modified for application to structured substrates. The process steps include (1) spin deposition of the LPP material onto the substrate followed by brief air-drying period, (2) irradiation with polarized 300-nm light from a 75-W xenon lamp passed through a Brewster's angle polarizer and a Schott UG-5 filter, and (3) a final bake step at 110°C to remove residual solvent.

Initially, spin-deposition of the LPP polymer onto the photoresist-structured substrates was problematic because of the generation of coating artifacts (ridges and ripples) in the vicinity of the diffraction element. These artifacts completely disrupted alignment of the LC material in the critical area around the diffracting element. This problem was solved by diluting the standard LPP coating solution with a compatible solvent with a slightly lower vapor pressure (cyclohexanone) to reduce the drying speed. Figure 14 shows the results obtained by spin-depositing the diluted LPP material onto a photoresist-structured ITO substrate.

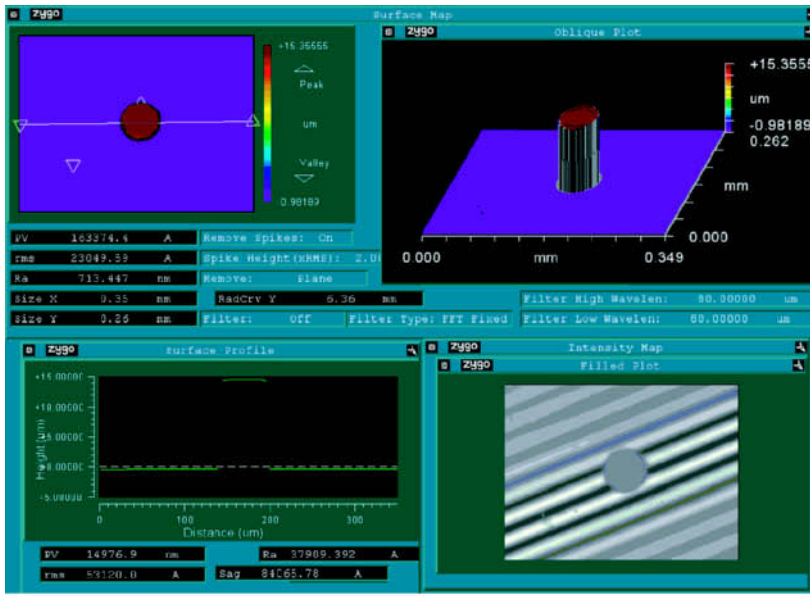

FIGURE 14 New View optical profilometer scans of a photoresist-structured substrate coated with LPP alignment material diluted to 25% LPP concentration. The area around the diffractive element is completely free of coating artifacts.

VI.D. Phase Shifting in "Second-Generation" LDPDI Devices

Structured substrates prepared using a photoresist, as described above in Secs. VI.B and VI.C, were used to assemble several second-generation LCPDI prototypes. The first prototype devices were prepared using one structured substrate and one "unstructured" substrate (containing only the ITO conductive coating and the LPP polymer alignment layer) because it proved to be very difficult to pattern both the central diffraction elements and the spacers in the photoresist in one step. Variations in the photoresist layer thickness near the edges of the substrates make it virtually impossible to obtain adequate height tolerances between the reference elements and the spacers. These initial devices were assembled in a similar manner to the first-generation LCPDI devices in that plastic microspheres dispersed in the UV-curing epoxy were used as both spacer pads and bonding elements to maintain tight contact between the integral structured referenced element and the unstructured second substrate. After they are filled with a contrast-compensated, dye-doped LC material, these devices were characterized using an interferometer setup with components similar to those shown in Figure 8, except that it employs 2-in.-diam optics and the optical path used a "folded" design that substantially reduced the footprint of the interferometer to a table area of around 28 in. by 28 in. [21]. The problem of producing structured substrates in which both the central diffractive elements and spacers have identical heights was solved using a two-step photoresist deposition and patterning operation, where the central diffractive elements were patterned and developed in the first step, followed by the subsequent deposition, patterning, and development of a second layer of photoresist that had been exposed through a second mask that contained openings only for the spacers. This

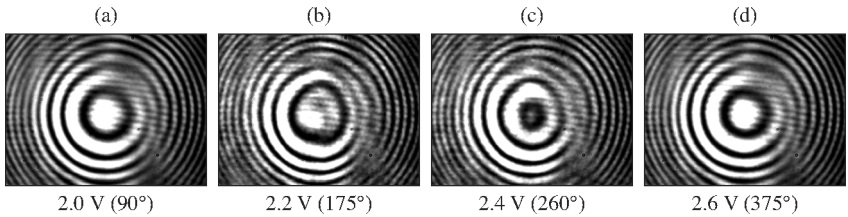

FIGURE 15 Phase-shifting interferograms collected using second-generation LDPDI modulation devices based on structured substrates. The interferometer was based on 2-in. optics and employed a "folded" optical path that reduced the interferometer's total footprint to an area of 28-in. × 28-in.

two-step process allows the heights of the central element and spacers to be varied independently and allows much tighter control of height tolerances between the diffraction elements and cell spacers. Figure 15 shows the phase-shifting interferograms collected from one of the most recent LCPDI devices employing these fully structured substrates.

VII. SUMMARY

Substantial progress toward the development of the LCPDI as a useful diagnostic tool has been made. Many of the key technology limitations have been identified and addressed in the course of this work. Guest–host dyes for both the visible region and the near IR were synthesized and their physical, chemical, and optical properties were evaluated in a commercial LC host mixture. Visible region LCPDI guest–host mixtures formulated using a combination of these dyes and existing commercial dichroic dyes were found to have low electrical conductivity, negligible electric field-induced absorbance dichroism, and excellent stability, thus eliminating the electrohydrodynamically induced speckle, voltage-dependent contrast, and poor molecular alignment stability observed in earlier LCPDI devices.

In conjunction with these new LC materials formulations, formation of reference-diffracting elements directly on the substrate surfaces was found to eliminate many of the assembly difficulties and performance limitations of first-generation LCPDI devices based on microspheres. The phase-shifting interferograms obtained using LCPCI devices containing these new mixtures along with substrates structured in photoresist are both clear evidence for the validity of the approach and a significant step toward the goal of making the LCPDI interferometer a viable alternative to conventional interferometers for challenging applications in the aerospace, military, security, and commercial sectors. Ongoing research efforts are concentrated on (1) extending the structured substrate concept to LCPDI modulators for near-IR interferometry applications and (2) the completion of driver electronics and user-friendly control software that will allow easy and rapid data acquisition and control with the export of data to standard interferometric packages for analysis and reduction.

REFERENCES

[1] Creath, K. (1988). In: *Progress in Optics XXVI*, Wolf, E. (Ed.), North-Holland: Amsterdam, Chap. V, 349.
[2] Mercer, C. R. & Creath, K. (1994). *Opt. Lett.*, *19*, 916.

[3] Mercer, C. R. & Creath, K. (1996). *Appl. Opt*., *35*, 1633.
[4] Mercer, C. R., Rashidnia, N., & Creath, K. (1996). *Exp. Fluids*, *21*, 11.
[5] Guardalben, M. J., Ning, L., Jain, N., Battaglia, D. J., & Marshall, K. L. (2002). *Appl. Opt*., *41*, 1353.
[6] Griffin, D. W. & Marshall, K. L. Phase-Shifting Liquid Crystal Interfereometers for Microgravity Fluid Physics, presented at the 6th Microgravity Fluid Physics and Transport Phenomena Conference, Cleveland, OH, 14–16 August 2002.
[7] Marshall, K. L., Klehn, B., Watson, B., & Griffin, D. W. (2003). In: *Advanced Characterization Techniques for Optics, Semiconductors, and Nanotechnologies*, Duparré, A. & Singh, B. (Eds.), SPIE: Bellingham, WA, Vol. 5188, 48.
[8] Kassemi, M. & Rashidnia, N. Dynamics of Oscillatory Thermocapillary and Natural Convection in Free Surface Problems, presented at the 37th Aerospace Sciences Meeting and Exhibit, Reno, NV, 11–14 January 1999 (AIAA Paper 99-0704).
[9] Kassemi, M. & Rashidnia, N. "Steady and Oscillatory Flows Generated by a Bubble in 1-G and Low-G Environments," presented at the 35th Aerospace Sciences Meeting and Exhibit, Reno, NV, 6–9 January 1997 (AIAA Paper 97-0924).
[10] Qiu, D. M., Dhir, V. K., Chao, D., Hasan, M. M., Neumann, E., Yee, G., & Birchenough, A. (2002). *J. Thermophys. Heat Transf*., *16*, 336.
[11] Rashidnia, N., Balasubramaniam, R., Kuang, J., Petijeans, P., & Maxworthy, T. (2001). *Int. J. Thermophys*., *22*, 547.
[12] McMackin, L., Hugo, R. J., Pierson, R. E., & Truman, C. R. (1997). *Opt. Express*, *1*, 302.
[13] Ivashchenko, A. V., Lazareva, V. T., Prudnikova, E. K., Rumyantsev, V. G., & Titov, V. V. (1985). *Mol. Cryst. Liq. Cryst*., *129*, 267.
[14] Ivashchenko, A. V. & Titov, V. V. (1991). *Mol. Cryst. Liq. Cryst*., *202*, 13.
[15] Prudnikova, E., Umanskii, B., & Plyusnina, T. (1999). *Mol. Cryst. Liq. Cryst*., *332*, 37.
[16] Marshall, K. L. & Jacobs, S. D. (1988). *Mol. Cryst. Liq. Cryst*., *159*, 181.
[17] Laboratory for Laser Energetics LLE Review *81*, 37, NTIS document No. DOE/SF/19460-335 (1999). Copies may be obtained from the National Technical Information Service, Springfield, VA 22161.
[18] Mueller-Westerhoff, U. T., Nazzal, A., Cox, R. J., & Giroud, A. M. (1980). *Mol. Cryst. Liq. Cryst. Lett*., *56*, 249.
[19] Ohta, K., Takagi, A., Muroki, H., Yamamoto, I., Matsuzaki, K., Inabe, T., & Maruyama, Y. (1987). *Mol. Cryst. Liq. Cryst*., *147*, 15.
[20] Marshall, K. L. U.S. Patent Application UR Docket #0209. (filed 13 September 2004).
[21] Marshall, K. L., Adelsberger, K., Kolodzie, B., Mhyre, G., & Griffin, D. W. A Second-Generation Liquid Crystal Phase-Shifting Point-Diffraction Interferometer Employing Structured Substrates," to be published in the Proceedings of SPIE's *Optics and Photonics 2005*.